

Theoretical Studies on Novel Main Group Metallocene-like Complexes Involving Planar Hexacoordinate Carbon $\eta^6\text{-B}_6\text{C}^{2-}$ Ligand

Qiong Luo,^{†,‡} Xiu Hui Zhang,[§] Ke Long Huang,[†] Su Qin Liu,[†] Zhong Heng Yu,[‡] and Qian Shu Li^{*,§}

School of Chemistry and Chemical Engineering, Central South University, Changsha 410083, People's Republic of China, Beijing National Laboratory for Molecular Sciences; State Key Laboratory for Structural Chemistry of Unstable & Stable Species, Institute of Chemistry, Chinese Academy of Sciences, Beijing 100080, People's Republic of China, and The Institute for Chemical Physics, Beijing Institute of Technology, Beijing 100081, People's Republic of China

Received: November 27, 2006; In Final Form: February 5, 2007

The geometric structures for a novel series of main group 1 and 2 metal atom complexes with planar hexacoordinate carbon dianion ($\eta^6\text{-B}_6\text{C}^{2-}$) ligand, involving metallocene-like, $\text{K}[(\eta^6\text{-B}_6\text{C})\text{Ca}]_n(\eta^6\text{-B}_6\text{C})\text{K}$ ($n = 1-3$) and $[(\eta^6\text{-B}_6\text{C})\text{Ca}]_n(\eta^6\text{-B}_6\text{C})^{2-}$ ($n = 1, 2$), as well as relative pyramidal $[(\eta^6\text{-B}_6\text{C})\text{M}]^{i-}$ ($\text{M} = \text{Na}, \text{K}$, and CaCl , $i = 1$; $\text{M} = \text{Ca}$, $i = 0$) and bipyramidal $(\eta^6\text{-B}_6\text{C})(\text{CaCl})_2$, have been optimized to be the local minima on the corresponding potential hypersurfaces at the B3LYP/6-311+G(d) level of theory. Natural bond orbital analysis indicates that the electrostatic interaction between the metal ions and the planar hexacoordinate carbon B_6C^{2-} rings plays a crucial role in stabilizing these highly symmetrical complexes. The π -d interaction in Ca-containing complexes also plays an important role in the stabilization of these molecules. It is found that the Ca^{2+} cation could be considered the best candidate for $(\eta^6\text{-B}_6\text{C})^{2-}$ to build ionic organometallic compounds. In these predicted multideck metallocene-like complexes there exist similarities in many structural properties, such as geometry parameters, Wiberg bond indices, natural atomic charges, atomic electronic configurations, and frontier orbital energies, as well as increments of the dissociation energy (to $-(\eta^6\text{-B}_6\text{C})\text{Ca}-$ units and metal cations) for adding one $-(\eta^6\text{-B}_6\text{C})\text{Ca}-$ unit and so on, which suggests that the $-(\eta^6\text{-B}_6\text{C})\text{Ca}-$ unit could be used as a building block to construct more $\text{K}[(\eta^6\text{-B}_6\text{C})\text{Ca}]_n(\eta^6\text{-B}_6\text{C})\text{K}$ chain-type metallocene-like complexes along their sixfold molecular axis.

I. Introduction

The exciting discovery of planar hexacoordinate carbon dianion (phC), D_{6h} B_6C^{2-} ,¹ with aromaticity makes a great contribution to carbon chemistry. It has been theoretically predicted that some transition metal atoms might engage the phC dianion, as six-electron π donors, to form metallocene-like compounds,² which implies that the novel aromatic dianion could develop a new field in coordination chemistry. In coordination chemistry, it is important to understand the interaction between ligands and all kinds of center atoms.³ The previous theoretical work on coordinating the phC dianion to transition metal atoms shows that the π -d interaction between the delocalized π B_6C^{2-} molecular orbitals and the d orbitals of the center transition metal ion plays a crucial role in stabilizing the compounds.² The function of B_6C^{2-} in those complexes is featureless and similar to many ligands in metallocene-like complexes.⁴⁻⁷ Li and his co-workers also predicted the structure of C_{6v} $[(\eta^6\text{-B}_6\text{C})\text{Li}]^{2-}$,² but the interaction between the ligand and the metal atom was left to be discussed.

It is known that D_{6h} B_6C^{2-} has a comparably redundant charge, -0.74 , populated on the planar hexacoordinate carbon atom.¹ This indicates that electropositive alkali and alkaline-earth atoms might be bound to phC B_6C^{2-} by electrostatic

interaction to form ionic complexes with high symmetry. To the best of our knowledge, detailed studies on main group metallocene-like complexes with the planar hexacoordinate carbon dianion B_6C^{2-} have not been reported to date. Therefore, this study focused on the complexes of the main group 1 and 2 atoms with phC B_6C^{2-} . Such novel highly symmetric organometallic complexes have been designed, including a series of compounds, metallocene-like $\text{K}[(\eta^6\text{-B}_6\text{C})\text{Ca}]_n(\eta^6\text{-B}_6\text{C})\text{K}$ ($n = 1-3$) and $[(\eta^6\text{-B}_6\text{C})\text{Ca}]_n(\eta^6\text{-B}_6\text{C})^{2-}$ ($n = 1, 2$), as well as relative pyramidal $[(\eta^6\text{-B}_6\text{C})\text{M}]^{i-}$ ($\text{M} = \text{Na}, \text{K}$, and CaCl , $i = 1$; $\text{M} = \text{Ca}$, $i = 0$) and bipyramidal $(\eta^6\text{-B}_6\text{C})(\text{CaCl})_2$, with metal ions located along the sixfold axis of B_6C^{2-} , and their stabilities have been predicted using the density functional method. The computational finding of multilayer sandwich-type complexes shows that the phC dianion B_6C^{2-} is also important to the development of coordination chemistry and organometallic chemistry.

II. Computational Details

Structural optimizations and frequency analyses for the main group metallocene-like pyramidal and bipyramidal complexes with the $\eta^6\text{-B}_6\text{C}^{2-}$ ligand under investigation along with the $\eta^6\text{-B}_6\text{C}^{2-}$ ligand were carried out using the hybrid density functional theory (DFT) method, which includes a mixture of Hartree-Fock exchange with density functional exchange correlation, denoted as B3LYP,⁸⁻¹⁰ with polarized split-valence basis sets, denoted as 6-311+G(d).¹¹⁻¹³ Natural bond orbital (NBO)¹⁴ analysis was also performed at the B3LYP/6-311+G-

* Corresponding author. Telephone: +86-10-68912665. Fax: +86-10-68912665. E-mail: qsl@bit.edu.cn.

[†] Central South University.

[‡] Chinese Academy of Sciences.

[§] Beijing Institute of Technology.

TABLE 1: Lowest Vibrational Frequencies (cm^{-1}), Selected Bond Lengths (\AA), Natural Atomic Charges (q), and Electronic Configuration (EC) of Metal Cations for All the Predicted Complexes

species	ν_{\min}	$r_{\text{B-B}}$	$r_{\text{B-C}}$	$r_{\text{C-M}}^a$	$r_{\text{C-Ca}}$	q_{c}	q_{M}^a	q_{Ca}	EC
$D_{6h} [\text{B}_6\text{C}]^{2-}$	269	1.593	1.593			-0.76			
$C_{6v} [(\text{B}_6\text{C})\text{Li}]^-$	298	1.585	1.600	1.972		-0.77	0.91		Li[He]2s ^{0.03} 4p ^{0.06}
$C_{6v} [(\text{B}_6\text{C})\text{Na}]^-$	122	1.590	1.594	2.356		-0.78	0.94		Na[Ne]3s ^{0.02} 3p ^{0.05}
$C_{6v} [(\text{B}_6\text{C})\text{K}]^-$	140	1.589	1.592	2.732		-0.77	0.96		K[Ar]4s ^{0.01} 3d ^{0.04} 4p ^{0.01}
$C_{6v} [(\text{B}_6\text{C})\text{Ca}]$	216	1.582	1.599		2.420	-0.76		1.69	Ca[Ar]4s ^{0.04} 3d ^{0.28}
$C_{6v} [(\text{B}_6\text{C})(\text{CaCl})]^-$	67	1.584	1.595		2.522	-0.76		1.76	Ca[Ar]4s ^{0.06} 3d ^{0.18} 4p ^{0.01}
$D_{6h} [(\text{B}_6\text{C})(\text{CaCl})_2]$	20	1.588	1.588		2.533	-0.96		1.78	Ca[Ar]4s ^{0.04} 3d ^{0.17} 4p ^{0.01}
$D_{6h} [(\text{B}_6\text{C})_2\text{Ca}]^{2-}$	0.6	1.585	1.594		2.631	-0.77		1.75	Ca[Ar]4s ^{0.07} 3d ^{0.17} 4p ^{0.01}
$D_{6h} [(\text{B}_6\text{C})_2\text{CaK}_2]$	10	1.586	1.589	2.744	2.559	-0.88	0.98	1.77	Ca[Ar]4s ^{0.06} 3d ^{0.17} 5p ^{0.01} K[Ar]3d ^{0.02}
$D_{6h} [(\text{B}_6\text{C})_3\text{Ca}_2]^{2-b}$	0.7i	1.584	1.595		2.557	-0.77		1.75	Ca[Ar]4s ^{0.07} 3d ^{0.17} 4p ^{0.01}
		1.587	1.587		2.617	-0.92			
$D_{6h} [(\text{B}_6\text{C})_3\text{Ca}_2\text{K}_2]^b$	10	1.586	1.589	2.752	2.539	-0.88	0.98	1.77	Ca[Ar]4s ^{0.06} 3d ^{0.17} 5p ^{0.01}
		1.587	1.587		2.549	-0.95			K[Ar]3d ^{0.02}
$D_{6h} [(\text{B}_6\text{C})_4\text{Ca}_3\text{K}_2]^b$	3i	1.586	1.589	2.756	2.533	-0.88	0.98	1.77	Ca[Ar]4s ^{0.06} 3d ^{0.17} 5p ^{0.01}
		1.587	1.587		2.554	-0.96		1.77	Ca[Ar]4s ^{0.06} 3d ^{0.17} 4p ^{0.01}
					2.528 ^c				K[Ar]3d ^{0.02}

^a M = Li, Na, or K. ^b The data are listed in the first line for the terminal B_6C rings or terminal Ca^{2+} cations and in the second line for the inner rings or inner Ca^{2+} cations. ^c The bond length between the center Ca atom and inner rings.

TABLE 2: Highest Occupied Molecular Orbital (HOMO) Energies (au), Energy Gap (Gap, in au) between the Highest Occupied and Lowest Unoccupied Orbitals, Dissociation Energies (Ed, in kcal/mol) to B_6C^{2-} Anions and Metal Cations, Wiberg Bond Indices (WBI) of Selected Bonds, and Nucleus-Independent Chemical Shifts (NICS, in ppm) of All the Predicted Complexes

species	HOMO	Gap	Ed	WBI _{C-M} ^a	WBI _{C-Ca}	WBI _{B-B}	WBI _{B-C}	NICS(0) ^b	NICS(+1) ^b	NICS(-1) ^b
$D_{6h} [\text{B}_6\text{C}]^{2-}$	0.15	0.08				1.26	0.64	73.1	-26.1	-26.1
$C_{6v} [(\text{B}_6\text{C})\text{Li}]^-$	-0.02	0.08	251.30	0.01		1.25	0.64	74.6	-36.1	-27.6
$C_{6v} [(\text{B}_6\text{C})\text{Na}]^-$	-0.01	0.06	217.18	0.01		1.25	0.64	78.7	-13.9	-33.1
$C_{6v} [(\text{B}_6\text{C})\text{K}]^-$	0	0.04	197.29	0.01		1.25	0.64	68.6	-20.3	-2.6
$C_{6v} [(\text{B}_6\text{C})\text{Ca}]$	-0.18	0.07	494.40		0.03	1.23	0.64	90.3	-10.9	-24.0
$C_{6v} [(\text{B}_6\text{C})(\text{CaCl})]^-$	-0.06	0.11	285.75		0.02	1.24	0.64	74.9	-24.1	-35.2
$D_{6h} [(\text{B}_6\text{C})(\text{CaCl})_2]$	-0.26	0.14	426.89		0.01	1.22	0.63	80.7	-33.4	-33.4
$D_{6h} [(\text{B}_6\text{C})_2\text{Ca}]^{2-}$	0.05	0.07	613.85		0.01	1.25	0.64	70.2	-33.5	-28.7
$D_{6h} [(\text{B}_6\text{C})_2\text{CaK}_2]$	-0.17	0.11	870.16	0.01	0.01	1.23	0.63	75.4	-32.9	-31.9
$D_{6h} [(\text{B}_6\text{C})_3\text{Ca}_2]^{2-c}$	0.01	0.09	1186.12		0.01	1.24	0.64	74.2	-34.9	-26.8
					0.01	1.22	0.63	69.7	-35.8	-35.8
$D_{6h} [(\text{B}_6\text{C})_3\text{Ca}_2\text{K}_2]^c$	-0.19	0.12	1416.17	0.01	0.01	1.23	0.63	77.1	-33.5	-31.2
					0.01	1.22	0.63	77.8	-35.5	-35.5
$D_{6h} [(\text{B}_6\text{C})_4\text{Ca}_3\text{K}_2]^c$	-0.19	0.10	1960.80	0.01	0.01	1.23	0.63	77.6	-30.0	-34.6
					0.01	1.22	0.63	79.3	-35.7	-35.4
					0.01 ^d					

^a M = Li, Na, or K. ^b ± 1 above/below the C atom by 1.0 \AA along the direction from the C atom to the metal atom for $C_{6v} [(\eta^6\text{-B}_6\text{C})\text{M}]^-$ (M = Li, Na, K, and CaCl, $i = 1$; M = Ca, $i = 0$), and along the direction from the molecular center to the terminal ring for the other compounds. ^c The data are listed in the first line for the terminal B_6C rings or Ca cations and in the second line for the inner rings or C atom. ^d The WBI between the center Ca atom and the C atoms in inner rings.

TABLE 3: Kitaura–Morokuma Energy Decomposition (kcal/mol) of $[(\text{B}_6\text{C})\text{Ca}]$ and $[(\text{B}_6\text{C})\text{K}]^-$ at the 6-311G(d) Basis Set^a

system	ΔE_{int}	ΔE_{elec}	ΔE_{ex}	$\Delta E_{\text{elec}} + \Delta E_{\text{ex}}$	ΔE_{pol}	ΔE_{ct}	ΔE_{mix}
$C_{6v} [(\text{B}_6\text{C})\text{Ca}]$	-462.14	-441.28	62.77	-378.51	-185.71	-256.35	358.43
$C_{6v} [(\text{B}_6\text{C})\text{K}]^-$	-196.56	-203.91	25.68	-178.23	-25.93	-147.34	154.94

^a BSSE is included.

(d) level of theory. All these calculations were implemented by using the Gaussian 03 program.¹⁵

An energy decomposition analysis at the HF/6-311G(d) level of theory was carried out, using the Kitaura–Morokuma (K–M) energy decomposition scheme in the quantum chemistry package GAMESS,^{16–18} to obtain a quantitative description about the electrostatic and π -d interactions between the metal atom and ligand(s) in $[(\eta^6\text{-B}_6\text{C})\text{Ca}]$ and $[(\eta^6\text{-B}_6\text{C})\text{K}]^-$. In the K–M scheme, the interaction energy ΔE_{int} between two fragments in the molecule can be divided into five components, including electrostatic energy ΔE_{elec} , exchange repulsion energy ΔE_{ex} , polarization energy ΔE_{pol} , charge-transfer energy ΔE_{ct} , and high order coupling energy ΔE_{mix} :

$$\Delta E_{\text{int}} = \Delta E_{\text{elec}} + \Delta E_{\text{ex}} + \Delta E_{\text{pol}} + \Delta E_{\text{ct}} + \Delta E_{\text{mix}}$$

III. Results and Discussion

Table 1 collects the lowest vibrational frequencies (ν_{\min}), selected bond lengths, natural atomic charges, and electronic configurations (EC) of metal cations for all the studied complexes. The highest occupied molecular orbital (HOMO) energies, energy gaps (Gap) between the highest occupied and the lowest unoccupied orbitals, dissociation energies (Ed) to the B_6C^{2-} anions and metal cations, selected Wiberg bond indices (WBI), and nucleus-independent chemical shifts (NICS)¹⁹ of all the predicted compounds are listed in Table 2. Table 3 shows the K–M energy decomposition of $[(\eta^6\text{-B}_6\text{C})\text{Ca}]$ and $[(\eta^6\text{-B}_6\text{C})\text{K}]^-$ at the 6-311G(d) basis set. The overviews of the structures for the predicted compounds are depicted in Figures 1 and 3. The four highest occupied molecular orbitals of $C_{6v} [(\eta^6\text{-B}_6\text{C})\text{Ca}]$ and $C_{6v} [(\eta^6\text{-B}_6\text{C})\text{K}]^-$ are plotted in Figure 2.

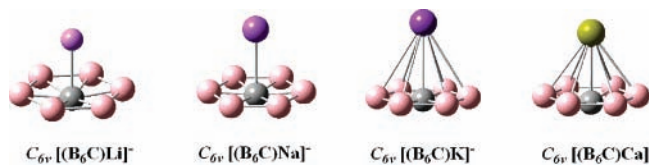


Figure 1. Optimized structures of C_{6v} $[(\eta^6\text{-B}_6\text{C})\text{M}]^-$ ($\text{M} = \text{Li}, \text{Na},$ and K) and C_{6v} $[(\eta^6\text{-B}_6\text{C})\text{Ca}]$. See Table 1 for selected structural parameters.

As shown in Figure 1, when one group 1 or 2 atom ($\text{M} = \text{Li}, \text{Na}, \text{K},$ and Ca) is bonded to a phC $\eta^6\text{-B}_6\text{C}^{2-}$ ring along its sixfold axis, a pyramidal structure with C_{6v} symmetry can be formed. These species are confirmed to be genuine minima by frequency analysis (see Table 1). However, efforts to optimize the geometries of C_{6v} $[(\eta^6\text{-B}_6\text{C})\text{Be}]$ and C_{6v} $[(\eta^6\text{-B}_6\text{C})\text{Mg}]$ are frustrated. In all these optimized C_{6v} symmetry structures, the B–B and B–C bond lengths are respectively close to those of $\eta^6\text{-B}_6\text{C}^{2-}$ calculated at the same level of theory with a difference of less than 0.01 Å. In all the above species, the six-membered B-rings are planar, and the C atom has a slight deviation from the B_6 plane, with the largest one of 0.23 Å in C_{6v} $[(\eta^6\text{-B}_6\text{C})\text{Ca}]$. The B_6C ring in the pyramidal structures can still be approximately regarded as quasi-phC.

The interaction between the new ligand and the metal cations has been studied by NBO analysis. For the alkali element compounds, the natural atomic charges of Li, Na, and K in C_{6v} $[(\eta^6\text{-B}_6\text{C})\text{M}]^-$ are 0.91, 0.94, and 0.96, respectively (see Table 1). This clearly demonstrates that the interaction between M^+ and B_6C^{2-} is a typical ionic bond. The small values of $\text{WBI}_{\text{C-M}}$ ($\text{M} = \text{Li}, \text{Na},$ and K), 0.01, confirm this estimation. The initial structures of B_6C^{2-} ligand are well maintained in these complexes, especially for C_{6v} $[(\eta^6\text{-B}_6\text{C})\text{K}]^-$ with the deviation between the C atom and the B_6 plane only 0.09 Å. This could be explained by the bond feature between the C and metal atoms. With the increase in atomic number of the alkali metals, the positive charge population on metals of these alkali complexes augments. Thus the C–K bond displays the strongest ionic interaction and the least covalent character, which leads to little influence of the metal cations on the structure of the ligand. It can be seen from Table 2 that the HOMO energies of C_{6v} $[(\eta^6\text{-B}_6\text{C})\text{M}]^-$ ($\text{M} = \text{Li}, \text{Na},$ and K) are $-0.02, -0.01,$ and 0.00 au, respectively, while that of the dianion $\eta^6\text{-B}_6\text{C}^{2-}$ is 0.15 au. Therefore, the dianion $\eta^6\text{-B}_6\text{C}^{2-}$ can be effectively stabilized by those group 1 metal atoms in forming complexes C_{6v} $[(\eta^6\text{-B}_6\text{C})\text{M}]^-$ ($\text{M} = \text{Li}, \text{Na},$ and K).

For C_{6v} $[(\eta^6\text{-B}_6\text{C})\text{Ca}]$, the natural atomic charges of C and Ca are -0.76 and $+1.69$, respectively, and $\text{WBI}_{\text{C-Ca}}$ is only 0.02 (see Table 2), indicating that the bond between C and Ca is also strong electrostatic interaction, though the positive charge on the Ca atom decreases compared to that on Ca^{2+} cation in traditional calcium salts, such as CaCl_2 . As shown in Figure 2, the molecular orbitals of C_{6v} $[(\eta^6\text{-B}_6\text{C})\text{Ca}]$ distinctly illustrate that the decrease of the positive charge on Ca atom results from the π –d back-donation from B_6C^{2-} to Ca^{2+} , while the homologous molecular d orbitals of K and π orbitals of B_6C^{2-} have little portions overlapping in C_{6v} $[(\eta^6\text{-B}_6\text{C})\text{K}]^-$. The natural atomic electronic configuration of Ca, $[\text{Ar}]4s^{0.04}3d^{0.28}$, suggests the π –d back-donation trend in C_{6v} $[(\eta^6\text{-B}_6\text{C})\text{Ca}]$.

Table 2 shows that the HOMO energy of C_{6v} $[(\eta^6\text{-B}_6\text{C})\text{Ca}]$ lies 0.16–0.18 au below that of C_{6v} $[(\eta^6\text{-B}_6\text{C})\text{M}]^-$ ($\text{M} = \text{Li}, \text{Na},$ and K). The dramatic differences between C_{6v} $[(\eta^6\text{-B}_6\text{C})\text{Ca}]$ and C_{6v} $[(\eta^6\text{-B}_6\text{C})\text{M}]^-$ are the embodiment of the π –d interaction in C_{6v} $[(\eta^6\text{-B}_6\text{C})\text{Ca}]$. Although the B_6C^{2-} – Ca^{2+}

interaction is mainly ionic, the π –d interaction is also considered to play an important role in the stabilization of C_{6v} $[(\eta^6\text{-B}_6\text{C})\text{Ca}]$.

The ionic radius of K is larger than that of Ca by nearly 0.5 Å, and the electronegativity of K^+ is smaller than that of Ca^{2+} . Therefore, the d orbitals of K^+ do not easily accept π electrons of B_6C^{2-} and K^+ , being different from Ca^{2+} , could not form a π –d interaction with B_6C^{2-} , although K⁺ has the same Ar core as Ca^{2+} . A detailed insight into the nature of the metal–ligand interactions of compounds $[(\eta^6\text{-B}_6\text{C})\text{Ca}]$ and $[(\eta^6\text{-B}_6\text{C})\text{K}]^-$ was given by the K–M energy decomposition analysis. As displayed in Table 3, their energy contributions of the electrostatic and π –d interactions between metal and ligand were quantitatively described. The Ca– B_6C interaction energy ΔE_{int} is significantly larger than the K– B_6C value by a factor of >2 . The leading term in the calculated ΔE_{int} are the electrostatic energies ΔE_{elec} , which are attenuated by the opposing term ΔE_{ex} , in both compounds. The ionic contributions to the bonding interactions given by the percentage of the $\Delta E_{\text{elec}} + \Delta E_{\text{ex}}$ in the ΔE_{int} term are 81.9% for $[(\eta^6\text{-B}_6\text{C})\text{Ca}]$ and 90.7% for $[(\eta^6\text{-B}_6\text{C})\text{K}]^-$. Though the energies ΔE_{pol} and ΔE_{ct} tend to be somewhat overestimated by the K–M analysis due to the presence of a relatively large coupling term ΔE_{mix} , the K–M results still suggest that both metal–ligand bonds are mainly ionic, and the bond of Ca– B_6C is more covalent than that of the K– B_6C bond. The more covalent content of the Ca– B_6C bond is associated with the π –d interaction between the metal and ligand.

Similarly, the reason stable C_{6v} $[(\eta^6\text{-B}_6\text{C})\text{Be}]$ and C_{6v} $[(\eta^6\text{-B}_6\text{C})\text{Mg}]$ compounds were not optimized successfully may be attributed to the lesser electropositivity of the Be and Mg atoms, compared with the alkali atoms, and the absence of d orbitals in the π –d interaction as performing in C_{6v} $[(\eta^6\text{-B}_6\text{C})\text{Ca}]$.

From the above studies, it can be assumed that Ca^{2+} is the best candidate for $\eta^6\text{-B}_6\text{C}^{2-}$ to form ionic organometallic compounds. Therefore, some new compounds based on the interaction between the Ca^{2+} cation and $\eta^6\text{-B}_6\text{C}^{2-}$ anion can be further constructed. At first, one and two CaCl^+ ions are tried to bond to $\eta^6\text{-B}_6\text{C}^{2-}$ along its sixfold axis to form C_{6v} $[(\eta^6\text{-B}_6\text{C})\text{CaCl}]^-$ and D_{6h} $[(\eta^6\text{-B}_6\text{C})(\text{CaCl})_2]$, respectively. The theoretical calculations predict that these two compounds are both local minima on their corresponding potential hypersurfaces. Their natural atomic charge populations of the Ca atom, 1.76 and 1.78, and WBI indices of the C–Ca bond, 0.02 and 0.01, are close to those, 1.69 and 0.03, of C_{6v} $[(\eta^6\text{-B}_6\text{C})\text{Ca}]$. The electronic configuration of Ca^{2+} ion is $[\text{Ar}]4s^{0.06}3d^{0.18}$ for C_{6v} $[(\eta^6\text{-B}_6\text{C})\text{CaCl}]^-$ and $[\text{Ar}]4s^{0.04}3d^{0.17}4p^{0.01}$ for D_{6h} $[(\eta^6\text{-B}_6\text{C})(\text{CaCl})_2]$, which show that the π –d interaction also exerts an influence on the stabilization of both complexes (see Table 2).

The detection of C_{6v} $[(\eta^6\text{-B}_6\text{C})\text{CaCl}]^-$ is significant, since it shows B_6C^{2-} can effectively bond to a Ca^{2+} cation as Cl^- does in CaCl_2 . Inspired by the finding, one B_6C^{2-} should be substituted for another Cl^- in C_{6v} $[(\eta^6\text{-B}_6\text{C})\text{CaCl}]^-$ to form a sandwich-type complex. An eclipsed D_{6h} $[(\eta^6\text{-B}_6\text{C})_2\text{Ca}]^{2-}$ structure has been optimized to be a local minimum. In the same way, the structure D_{6h} $[(\eta^6\text{-B}_6\text{C})_3\text{Ca}]^{2-}$, by replacing Cl^- with B_6C^{2-} for D_{6h} $[(\eta^6\text{-B}_6\text{C})(\text{CaCl})_2]$, has also been optimized. This structure has one imaginary frequency of $0.7i$ cm^{-1} . Schaefer has pointed out that low-magnitude imaginary vibrational frequencies are suspect because the numerical integration procedures used in existing DFT methods have significant limitations. Thus, an imaginary vibrational frequency of magnitude less than 100 cm^{-1} should imply that there is a minimum with energy very similar to that of the stationary point in question. In most cases, we do not follow the eigenvectors

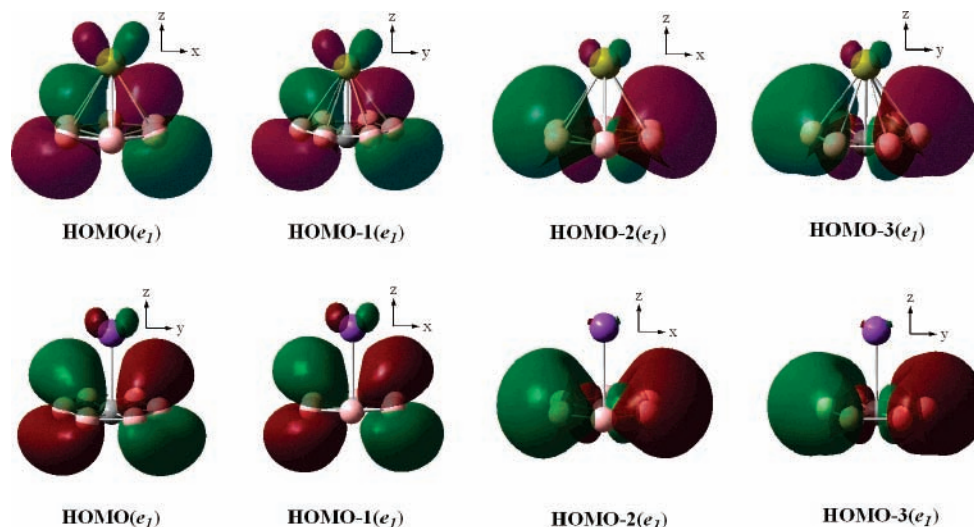


Figure 2. The four highest occupied molecular orbitals of C_{6v} $[(\eta^6\text{-B}_6\text{C})\text{Ca}]$ and C_{6v} $[(\eta^6\text{-B}_6\text{C})\text{K}]^-$.

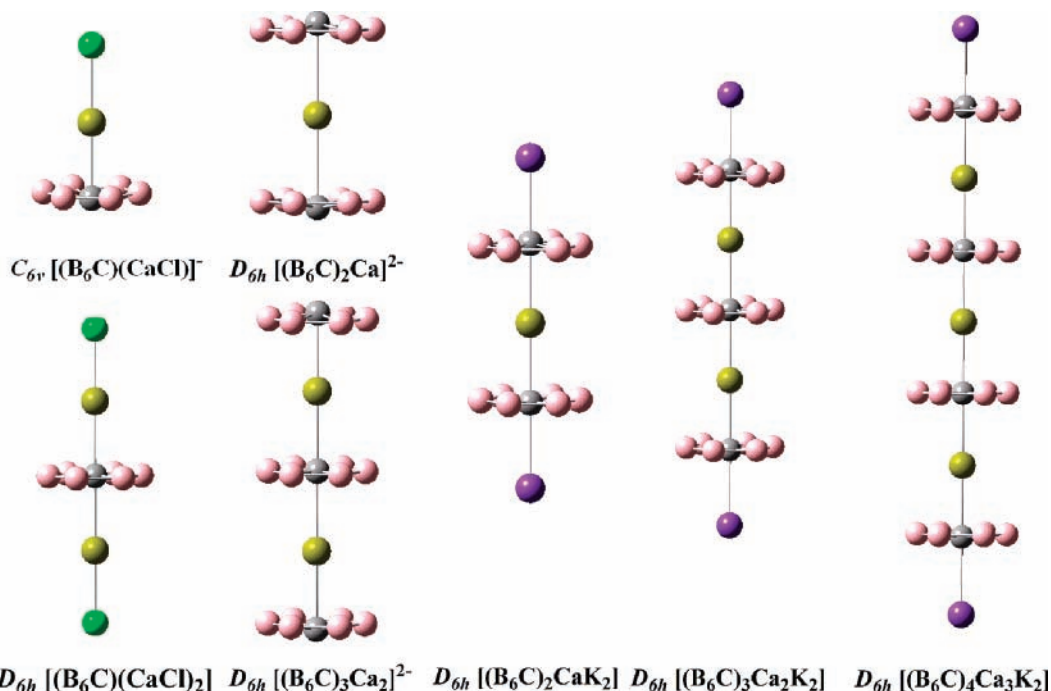


Figure 3. Optimized structures of C_{6v} $[(\eta^6\text{-B}_6\text{C})\text{CaCl}]^-$, D_{6h} $[(\eta^6\text{-B}_6\text{C})(\text{CaCl})_2]$, D_{6h} $[(\eta^6\text{-B}_6\text{C})_{n+1}\text{Ca}_n]^{2-}$ ($n = 1$ and 2), and D_{6h} $[(\eta^6\text{-B}_6\text{C})_{n+1}\text{Ca}_n\text{K}_2]$ ($n = 1, 2$, and 3). See Table 1 for selected structural parameters.

corresponding to imaginary frequencies less than $100i\text{ cm}^{-1}$ in search of another minimum.^{20,21} Therefore, the structure of D_{6h} $[(\eta^6\text{-B}_6\text{C})_3\text{Ca}_2]^{2-}$ could still be identified as a local minimum. The structures of both compounds can be viewed in Figure 3.

As exhibited in Table 2, D_{6h} $[(\eta^6\text{-B}_6\text{C})_3\text{Ca}_2]^{2-}$ and D_{6h} $[(\eta^6\text{-B}_6\text{C})_2\text{Ca}]^{2-}$ are unstable toward electron dissociation due to their HOMOs with positive energies. To reduce the HOMO energies, two K^+ ions are attempted to bind respectively to the two terminal rings of D_{6h} $[(\eta^6\text{-B}_6\text{C})_2\text{Ca}]^{2-}$ and D_{6h} $[(\eta^6\text{-B}_6\text{C})_3\text{Ca}_2]^{2-}$, along the molecular sixfold axis. The two local minima, D_{6h} $[(\eta^6\text{-B}_6\text{C})_2\text{CaK}_2]$ and D_{6h} $[(\eta^6\text{-B}_6\text{C})_3\text{Ca}_2\text{K}_2]$, have been theoretically predicted with the calculated lowest frequency located at 10 cm^{-1} , and their HOMO energies are -0.17 and -0.19 au , respectively.

Since CaCl^+ is isovalence electronic with K^+ , it could be supposed that CaCl^+ might be substituted for K^+ in both D_{6h} $[(\eta^6\text{-B}_6\text{C})_2\text{CaK}_2]$ and D_{6h} $[(\eta^6\text{-B}_6\text{C})_3\text{Ca}_2\text{K}_2]$; then the Cl^- is replaced by B_6C^{2-} , and thus multideck organometallic com-

plexes could be constructed. To prove the guess, the structure of D_{6h} $[(\eta^6\text{-B}_6\text{C})_4\text{Ca}_3\text{K}_2]$ has also been optimized. Similarly, the optimized structure could still be identified as a local minimum with the lowest frequency of $3i\text{ cm}^{-1}$.

Comparing the three predicted complexes, D_{6h} $[(\eta^6\text{-B}_6\text{C})_{n+1}\text{Ca}_n\text{K}_2]$ ($n = 1, 2$, and 3), from Tables 1 and 2, it could be found that, with the increase of n , (1) their corresponding geometry parameters are the same for $r_{\text{B-B}}$ and $r_{\text{B-C}}$, and slowly increase for $r_{\text{C-K}}$, while slowly decreasing for $r_{\text{C-Ca}}$; (2) their Wiberg bond indices ($\text{WBI}_{\text{C-Ca}}$, $\text{WBI}_{\text{C-K}}$, $\text{WBI}_{\text{B-B}}$, and $\text{WBI}_{\text{B-C}}$) and natural atomic charges (q_{C} , q_{K} , and q_{Ca}), as well as electronic configurations (EC) of Ca^{2+} and K^+ cations are all the same; and (3) their HOMO and Gap energies, as well as increment of the dissociation energy E_d for adding one $-(\eta^6\text{-B}_6\text{C})\text{Ca}-$ unit, are all close to each other. This implies that the $-(\eta^6\text{-B}_6\text{C})\text{Ca}-$ unit in the predicted complexes is relatively independent and could be utilized as a building block to construct $\text{K}[(\eta^6\text{-B}_6\text{C})\text{Ca}]_n(\eta^6\text{-B}_6\text{C})\text{K}$ chains along its sixfold molecular axis.

In all the compounds studied here, the phC B₆C²⁻ rings have structural and bond properties in common. The predicted bond lengths of r_{B-B} (1.582–1.590 Å) and r_{B-C} (1.585–1.600 Å) in all predicted complexes are very close to those of B₆C²⁻ (1.593 Å). The calculated WBI_{B-B} (1.22–1.25) and WBI_{B-C} (0.63–0.64) are also very similar to those of B₆C²⁻ (1.26 and 0.64) (see Table 2), indicating that the B–B and B–C bonds in these main group organometallic complexes are as well held as those in B₆C²⁻. The aromaticities of the B₆C²⁻ rings in these compounds are revealed by NICS.¹⁵ NICS(0) and NICS(±1) for B₆C in the compounds are listed in Table 2, in which the numbers in parentheses stand for the position of the ghost atom relative to the center C atom: 0 on the C atom and ±1 above/below the C atom by 1.0 Å along the direction from the C atom to the metal atom for C_{6v} [(η⁶-B₆C)M]ⁱ⁻ (M = Li, Na, K, and CaCl, *i* = 1; M = Ca, *i* = 0), and along the direction from the molecular center to the terminal ring for the other compounds. The calculated values of NICS(0) are all positive, while those of NICS(±1) are all negative, which shows that the rings are of π aromaticity with the contributions from the 6π electrons provided by boron atoms, which is similar to the case of B₆C²⁻.

IV. Summary

A novel series of main group metal complexes with planar hexacoordinate carbon η⁶-B₆C²⁻ ligand, including metallocene-like K[(η⁶-B₆C)Ca]_{*n*}(η⁶-B₆C)K (*n* = 1–3) and [(η⁶-B₆C)Ca]_{*n*}(η⁶-B₆C)²⁻ (*n* = 1, 2) as well as relative pyramidal [(η⁶-B₆C)M]ⁱ⁻ (M = Na, K, and CaCl, *i* = 1; M = Ca, *i* = 0) and bipyramidal (η⁶-B₆C)(CaCl)₂, are predicted to be local minima on their corresponding potential hypersurfaces at the B3LYP/6-311+G(d) level of theory. The chemical bond analysis indicates that the electrostatic interaction between the metal cations and the C_{6v} B₆C²⁻ rings is the key factor for the stabilization of the complexes. The lack of C_{6v} [(η⁶-B₆C)Be] and C_{6v} [(η⁶-B₆C)Mg] suggests that the π–d interaction in C_{6v} [(η⁶-B₆C)Ca] also plays an important role in stabilizing the compound. Due to electropositivity and the existence of π–d interaction, the Ca²⁺ cation is predicted to be the best candidate for (η⁶-B₆C)²⁻ to build ionic organometallic compounds. A series of metallocene-like complexes involving Ca cation(s) coordinated by two, three, or four (η⁶-B₆C)²⁻ ligands, K[(η⁶-B₆C)Ca]_{*n*}(η⁶-B₆C)K (*n* = 1–3), are optimized to be local minima on their corresponding potential surfaces at the same level of theory. Their corresponding geometric parameters, Wiberg bond indices, natural atomic charges, atomic electronic configurations, and frontier orbital energies, as well as increment of the dissociation energy (to –[(η⁶-B₆C)Ca]– units and metal cations) for adding one –[(η⁶-B₆C)Ca]– unit, are all very close

to each other. This fact makes us believe that the –[(η⁶-B₆C)Ca]– unit in the predicted complexes is relatively independent and could be applied as a building block to form more metallocene-like K[(η⁶-B₆C)Ca]_{*n*}(η⁶-B₆C)K complexes having sixfold axis symmetry.

Acknowledgment. This work was supported by the 111 Project (B07012) in the People's Republic of China.

References and Notes

- (1) Exner, K.; Schleyer, P. v. R. *Science* **2000**, *290*, 1937.
- (2) Li, S.-D.; Guo, J.-C.; Miao, C.-Q.; Ren, G.-M. *Angew. Chem., Int. Ed.* **2005**, *44*, 2158.
- (3) Jutzi, P.; Burford, N. *Chem. Rev.* **1999**, *99*, 969.
- (4) Haaland, A. *Acc. Chem. Res.* **1979**, *12*, 415.
- (5) Frunzke, J.; Lein, M.; Frenking, G. *Organometallics* **2002**, *21*, 3351.
- (6) Lein, M.; Frunzke, J.; Timoshkin, A.; Frenking, G. *Chem.–Eur. J.* **2001**, *7*, 4155.
- (7) Tsiapis, A. C.; Chaviara, A. T. *Inorg. Chem.* **2004**, *43*, 1273.
- (8) Becke, A. D. *J. Chem. Phys.* **1993**, *98*, 5648.
- (9) Lee, C.; Yang, W.; Parr, R. G. *Phys. Rev. B* **1988**, *37*, 785.
- (10) Perdew, J. P.; Chevary, J. A.; Vosko, S. H.; Jackson, K. A.; Pederson, M. R.; Singh, D. J.; Fiolhais, C. *Phys. Rev. B* **1992**, *46*, 6671.
- (11) McLean, A. D.; Chandler, G. S. *J. Chem. Phys.* **1980**, *72*, 5639.
- (12) Clark, T.; Chandrasekhar, J.; Spitznagel, G. W.; Schleyer, P. v. R. *J. Comput. Chem.* **1983**, *4*, 294.
- (13) Frisch, M. J.; Pople, J. A.; Binkley, J. S. *J. Chem. Phys.* **1984**, *80*, 3265.
- (14) Carpenter, J. E.; Weinhold, F. *J. Mol. Struct.* **1988**, *169*, 41.
- (15) Frisch, M. J.; Trucks, G. W.; Schlegel, H. B.; Scuseria, G. E.; Robb, M. A.; Cheeseman, J. R.; Montgomery, J. A., Jr.; Vreven, T.; Kudin, K. N.; Burant, J. C.; Millam, J. M.; Iyengar, S. S.; Tomasi, J.; Barone, V.; Mennucci, B.; Cossi, M.; Scalmani, G.; Rega, N.; Petersson, G. A.; Nakatsuji, H.; Hada, M.; Ehara, M.; Toyota, K.; Fukuda, R.; Hasegawa, J.; Ishida, M.; Nakajima, T.; Honda, Y.; Kitao, O.; Nakai, H.; Klene, M.; Li, X.; Knox, J. E.; Hratchian, H. P.; Cross, J. B.; Adamo, C.; Jaramillo, J.; Gomperts, R.; Stratmann, R. E.; Yazyev, O.; Austin, A. J.; Cammi, R.; Pomelli, C.; Ochterski, J. W.; Ayala, P. Y.; Morokuma, K.; Voth, G. A.; Salvador, P.; Dannenberg, J. J.; Zakrzewski, V. G.; Dapprich, S.; Daniels, A. D.; Strain, M. C.; Farkas, O.; Malick, D. K.; Rabuck, A. D.; Raghavachari, K.; Foresman, J. B.; Ortiz, J. V.; Cui, Q.; Baboul, A. G.; Clifford, S.; Cioslowski, J.; Stefanov, B. B.; Liu, G.; Liashenko, A.; Piskorz, P.; Komaromi, I.; Martin, R. L.; Fox, D. J.; Keith, T.; Al-Laham, M. A.; Peng, C. Y.; Nanayakkara, A.; Challacombe, M.; Gill, P. M. W.; Johnson, B.; Chen, W.; Wong, M. W.; Gonzalez, C.; Pople, J. A. *Gaussian 03*; Gaussian, Inc.: Pittsburgh, PA, 2003.
- (16) Kitaura, K.; Morokuma, K. *Int. J. Quantum Chem.* **1976**, *10*, 325.
- (17) Morokuma, K.; Kitaura, K. In *Chemical Applications of Electrostatic Potentials*; Politzer, P., Truhlar, D. G., Eds.; Plenum Press: New York, NY, 1981; p 215.
- (18) Granovsky, A. A. PC GAMESS, version 7.0; <http://classic.chem.msu.gran/gamess/index.html>.
- (19) Schleyer, P. v. R.; Maerker, C.; Dransfeld, A.; Jiao, H.; Eikema-Hommes, N. J. R. v. *J. Am. Chem. Soc.* **1996**, *118*, 6317.
- (20) Xie, Y.; Schaefer, H. F.; King, R. B. *J. Am. Chem. Soc.* **2000**, *122*, 8746.
- (21) Wang, H.; Xie, Y.; King, R. B.; Schaefer, H. F. *Inorg. Chem.* **2006**, *45*, 5621.